

Supporting Information

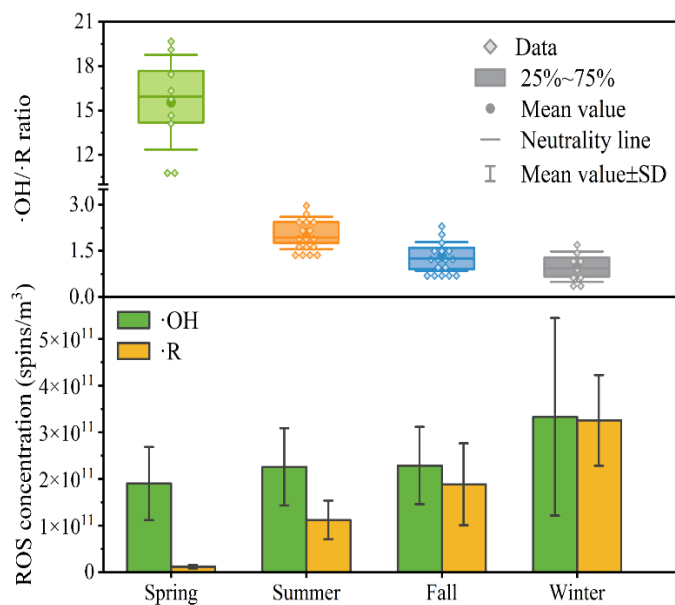


Fig. S1 Comparative ROS ($\cdot\text{OH}$, $\cdot\text{R}$) Concentrations and $\cdot\text{OH}/\cdot\text{R}$ Ratios in Seasonal Samples.

(Note: ROS ($\cdot\text{OH}$, $\cdot\text{R}$) indicates hydroxyl radicals and organic radicals. $\cdot\text{OH}/\cdot\text{R}$ ratios represent the concentration ratio of hydroxyl radicals to organic radicals.)

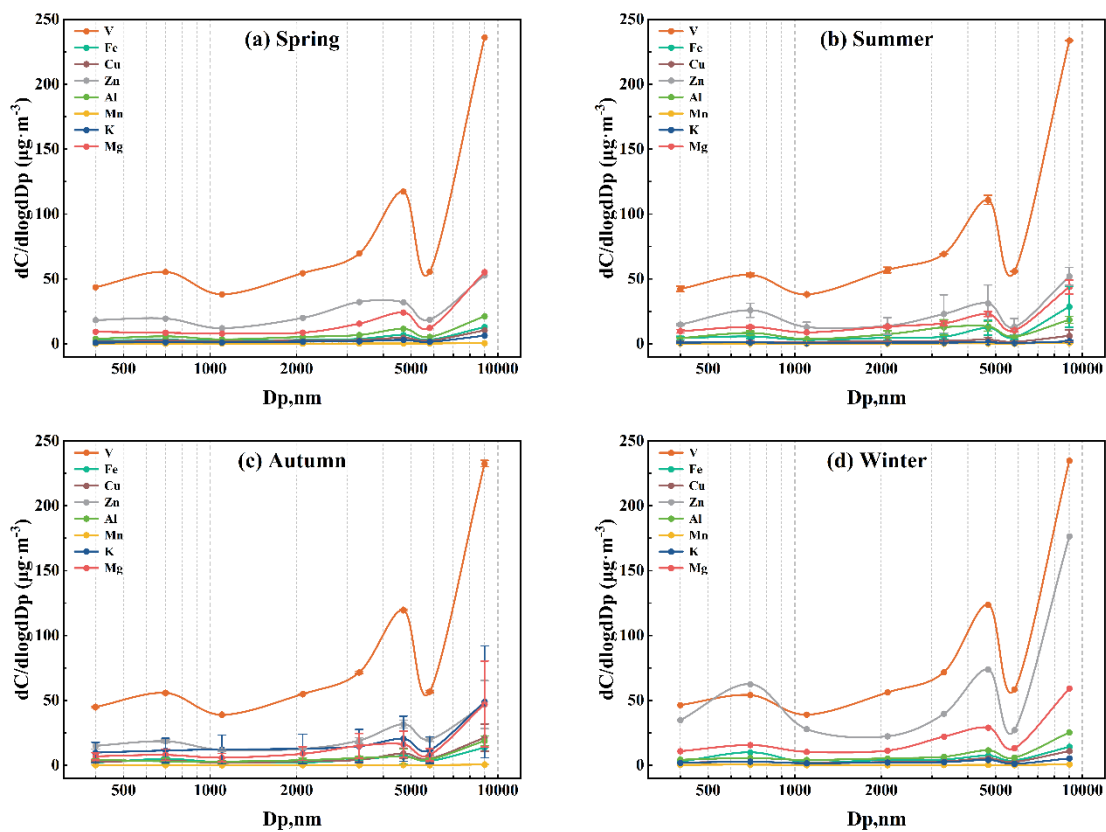


Fig. S2 Average size-resolved elemental distributions of outdoor airborne particles sampled across four seasons. $n = 52$, average \pm SD. (a) spring; (b) summer; (c) Autumn; (d) winter.

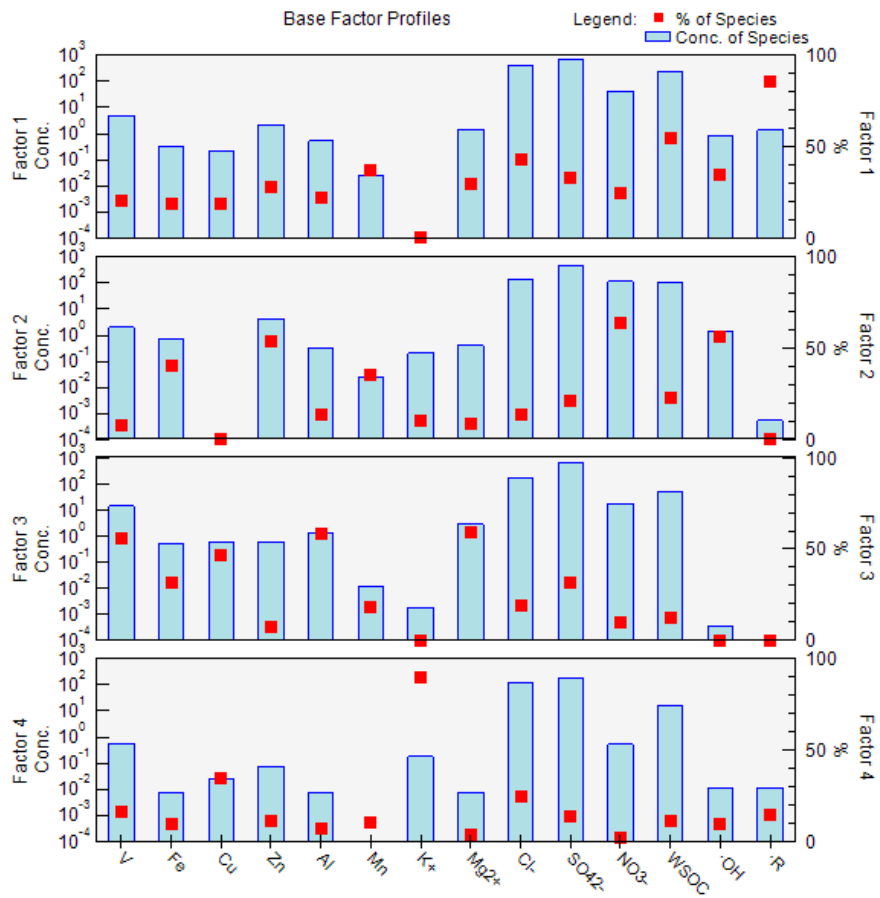


Fig. S3 Source profiles identified by Positive Matrix Factorization (PMF). (Note: based on all PM₁₀ samples across all seasons, n = 52; source: EPA PMF 5.0 software.)

Table S1 Impacts of Ambient particulate matter on Humans and Microorganisms.

Particulate Matter Dose	Human Impact	Microbial Impact	Reference
>10 $\mu\text{g}/\text{m}^3$ (chronic)	Neurodegeneration (AD, PD)	Gut dysbiosis	Liu et al., 2022b
≥ 30 $\mu\text{g}/\text{m}^3$	Genetic mutations	Metabolic disruption	Wei et al., 2016
50 $\mu\text{g}/\text{m}^3$	Mitochondrial damage	Pathogen proliferation	Xie et al., 2021
50 $\mu\text{g}/\text{mL}$	Cell viability decline	Not mentioned	Li et al., 2021
100 $\mu\text{g}/\text{mL}$	Pyroptotic cell death	Not mentioned	Li et al., 2021

(Note: AD, Alzheimer's Disease; PD, Parkinson's Disease)

Table S2 Seasonal Meteorological Conditions and Sampling Periods.

No	Sampling Period	Temperature (°C)	Wind Speed (m/s)	Humidity (%)
1	Spring 2022/02/25–2022/03/06 8:00–20:00	17.01±2.35	2.68±0.71	78.00±8.83
2	Summer 2022/06/22– 2022/07/01 8:00–20:00	28.35±0.55	2.65±0.44	79.30±3.06
3	Summer 2022/09/11– 2022/09/20 8:00–20:00	28.13±0.78	2.33±0.60	71.00±9.23
4	Fall 2022/10/11–2022/10/20 8:00–20:00	23.05±2.32	5.33±0.87	56.10±5.93
5	Fall 2022/11/10–2022/11/19 8:00–20:00	23.03±1.11	2.36±0.74	76.90±5.70
6	Winter 2022/12/20–2022/12/29 8:00–20:00	13.34±1.68	3.28±0.93	59.80±9.07

(Note: Data source: China Meteorological Data Service Center)

Table S3 Wavelength (cm^{-1}) for identification of major functional groups in Fourier transform infrared measurement.

Wavelength (cm^{-1})	Band assignments
3434	Stretching vibration of O–H
3320	O–H stretching of water
3131	Stretching mainly of O–H bond and/or amines, amides N–H
2955	Stretching vibration of aliphatic C–H
1724	Stretching mainly of carboxyl compounds C=O
1631	Stretching of aromatic C=C and ketones, quinones, and amides C=O
1102	Stretching of ring breathing C–O
1050	Stretching of polysaccharides C–O

Table S4 Size-resolved Particle Mass Distribution Collected by the Andersen Eight-stage Cascade Impactor (TE-20-800, Tisch, USA).

Stage	TARE (g)*	Final (g)	Net (mg)	% in size range	Cumulative % less than size range	Size range micrometers	ECD micrometers
Pre- separator	0	0.00009	0.09	(0.7)	98.7	10.0 & above	10.0
0	1.000	1.00009	0.09	(0.6)		9.0 – 10.0	9.0
1	1.000	1.00017	0.17	(1.2)	97.5	5.8 – 9.0	5.8
2	1.000	1.00082	0.82	5.7	91.8	4.7 – 5.8	4.7
3	1.000	1.00194	1.94	13.6	78.2	3.3 – 4.7	3.3
4	1.000	1.00472	4.72	33.1	45.1	2.1 – 3.3	2.1
5	1.000	1.00431	4.31	30.2	14.9	1.1 – 2.1	1.1
6	1.000	1.00100	1.00	7.0	7.9	0.7 – 1.1	0.7
7	1.000	1.00082	0.82	5.7	2.2	0.4 – 0.7	0.4
Backup Filter	1.000	1.00031	0.31	2.2	0	0 – 0.4	0
			14.27				

Text S1. Positive Matrix Factorization Factor Identification.

As shown in Fig. S3, four major source factors were identified. Traffic sources and secondary pollution were the predominant contributors to major metals (Fe, Mn, V, and Zn), WSOC, and major ions (NO_3^- and SO_4^{2-}). Factor 1 was identified as traffic source, characterized by significant levels of Mn (37%), Zn (28%), and Cu (19%), which are typical markers of brake and tire wear as well as vehicular abrasion. Zn, in particular, is widely used as an additive in automotive engine lubricants (Srivastava et al, 2021; Yao et al, 2016; Huang et al, 2018). Factor 2 was attributed to secondary source, with high proportions of NO_3^- (64%) and SO_4^{2-} (22%), mainly resulting from gas-to-particle conversion processes driven by atmospheric oxidation. The elevated WSOC (56%) suggests substantial secondary organic aerosol formation, likely influenced by VOC emissions and intensified traffic activities during peak tourism seasons, while WSOC was also primarily emitted by vehicles and ships burning gasoline and diesel in coastal megacities (Ding et al., 2019; Tang et al., 2016). The presence of V in vehicle emissions (14%) further aligns with its association with cargo ships and diesel vehicles, supporting the component analysis results (Srivastava et al., 2021; Yao et al., 2016). Factor 3 is related to dust source, characterized by high levels of Al (59%), Fe (32%), and Mg^{2+} (59%), consistent with contributions from soil, road dust, and construction activities. Additionally, Zn (8%) and Cu (50%) suggest industrial contributions, particularly from metal processing and construction materials. Factor 4 is linked to combustion source due to the high proportions of K^+ (87%) and Cl^- (21%), indicative of biomass burning, while V (14%) suggests an influence from heavy oil combustion, likely associated with agricultural activities and maritime emissions.

References

- Ding X, Qi J, Meng X. Characteristics and sources of organic carbon in coastal and marine atmospheric particulates over East China[J]. *Atmos. Res.*, 2019, 228: 281—291.
- Huang C, Hu Q, Wang H, et al. Emission factors of particulate and gaseous compounds from a large cargo vessel operated under real-world conditions[J]. *Environ. Pollut.*, 2018, 242: 667—674.
- Li L, Xing C, Zhou J, et al. Airborne particulate matter (PM_{2.5}) triggers ocular hypertension and glaucoma through pyroptosis[J]. *Part. Fibre Toxicol.*, 2021, 18: 1-13.
- Liu C, She Y, Huang J, et al. HMGB1-NLRP3-P2X7R pathway participates in PM_{2.5}-induced hippocampal neuron impairment by regulating microglia activation[J]. *Ecotoxicol. Environ. Saf.*, 2022b, 239: 113664.
- Srivastava D, Xu J, Vu T V, et al. Insight into PM_{2.5} sources by applying positive matrix factorization (PMF) at an urban and rural site of Beijing[J]. *Atmos. Chem. Phys. Discuss.*, 2021, 2021: 1—51.
- Tang X, Zhang X, Wang Z, et al. Water-soluble organic carbon (WSOC) and its temperature-resolved carbon fractions in atmospheric aerosols in Beijing[J]. *Atmos. Res.*, 2016, 181: 200-210.
- Wei H, Liang F, Meng G, et al. Redox/methylation mediated abnormal DNA methylation as regulators of ambient fine particulate matter-induced neurodevelopment related impairment in human neuronal cells[J]. *Sci. Rep.*, 2016, 6(1): 33402.
- Xie W, You J, Zhi C, et al. The toxicity of ambient fine particulate matter (PM_{2.5}) to vascular endothelial cells[J]. *J. Appl. Toxicol.*, 2021, 41(5): 713-723.
- Yao L, Yang L, Yuan Q, et al. Sources apportionment of PM_{2.5} in a background site in the North China Plain[J]. *Sci. Total Environ.*, 2016, 541: 590—598.